2. Materials and Methods

Aluminophosphate materials were used as catalysts in this study for various reactions. In particular, AlPO-5, SAPO-5, SAPO-34 and VPI-5 aluminophosphate zeotypes were used. Cobalt and Manganese substituted forms of these zeotypes were used which were prepared by the hydrothermal method in presence of salts (acetate or nitrate) of these metals. These materials were characterized by X-Ray diffraction (crystallinity and phase identification), Scanning electron microscopy (crystal structure and morphology determination), N_2-BET surface area measurement (surface area and pore size determination), Energy dispersive spectroscopy (quantitative analysis of elemental composition) and Fourier transform infrared spectroscopy (FTIR) to determine the chemical bonding and nature of acidic sites.

2.1 General information

2.1.1 AlPO-5

This aluminophosphate has AFI framework structure (Fig. 2.1.1) which is unique in terms of having no analogue of aluminosilicate type materials. This aluminophosphate has 12 T ring pore structure and one dimensional channel in its framework thorough which molecules may pass however the other pores present in the structure are small.

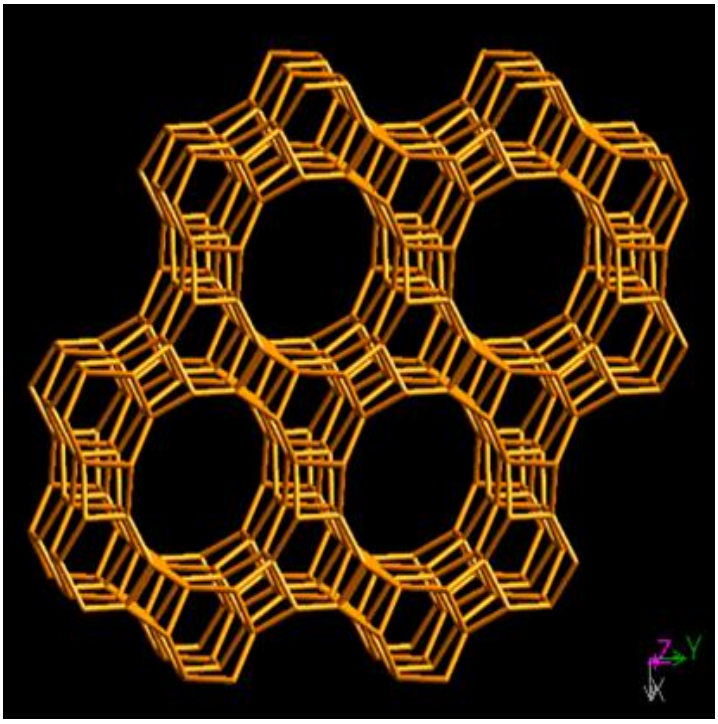

Fig. 2.1.1. 3D framework structure and channel system of AlPO-5 aluminophosphate

General information and crystallographic parameters are as follow:

AlPO-5*			
Parameter	**Description**		
Material	AlPO-5		
Category	Aluminophosphate		
Molar Composition	$\|(C_{12}H_{28}N^+)\ (OH^-)\ (H_2O)_x\ \|[Al_{12}P_{12}\ O_{48}]$		
Framework Type	AFI		
Crystallography			
Space group	P6/mcc		
Cell parameters	*a* = 13.827 Å	*b* = 13.827 Å	*c* = 8.580 Å
	α = 90.000 °	β = 90.000 °	γ= 120.000°
Volume	1420.64 $Å^3$		
R_{DLS}	0.0038		
Framework density	16.9 T/1000 $Å^3$		
Channel system	1dimensional		
Topological density	TD_{10} = 828 TD = 0.700000		
Ring sizes (T atoms)	12 6 4		
Maximum diameter of a sphere			
that can be included	8.30 Å		
that can diffuse along	a: 2.22 Å b: 2.22 Å c: 7.42 Å		

2.1.2 SAPO-5

This aluminophosphate has same framework structure as AlPO-5 i.e. AFI type. However, when silicon is inserted in its framework, few changes are observed in the framework topology. Due to the presence of silicon, synthesis chemistry of crystallization is affected too much and this structure shows different properties comparatively due to the presence of inserted silicon. General information and crystallography of SAPO-5 are same as that of AlPO-5. Chemical Formula is as follow:

$$[Al_{12}P_{12}Si_{12}\ O_{72}]|(C_{12}H_{28}N^+)\ (OH^-)\ (H_2O)_x\ |$$

2.1.3 SAPO-34

SAPO-34 has CHA framework structure which is an analogue of chabazite aluminosilicate zeolite. Crystallographic information is as follows:

SAPO-34*			
Parameter	**Description**		
Material	SAPO-34		
Category	Silicoaluminophosphate		
Molar Composition	$\|12H^{+}(H_2O)_{40}\|$ **[**$Al_{12}Si_{24}O_{72}$**]**		
Framework Type	CHA		
Crystallography			
Space group	R-3m		
Cell parameters	*a* = 9.42Å	*b* = 9.42Å	*c* = 9.42 Å
	α = 94.47 °	β = 94.47 °	γ = 94.47 °
Volume	2391.59 $Å^3$		
R_{DLS}	0.0015		
Framework density	15.1 T/1000 $Å^3$		
Channel system	3-dimensional		
Topological density	TD_{10} = 677 TD = 0.566667		
Ring sizes (T atoms)	8 6 4		
Maximum diameter of a sphere			
that can be included	7.37 Å		
that can diffuse along	a: 3.72 Å b: 3.72 Å c: 3.72 Å		

From structure point of view, this material has great value for the cracking of small molecules or in catalysis because this zeotype has 3-dimentional pore channels intersecting each other. However, pore channel system is smaller in size thus only small molecules penetrate it. Additionally, its framework structure (Fig. 2.1.2) is so different than that of other aluminophosphates that it can capture or include more amounts of molecules within it.

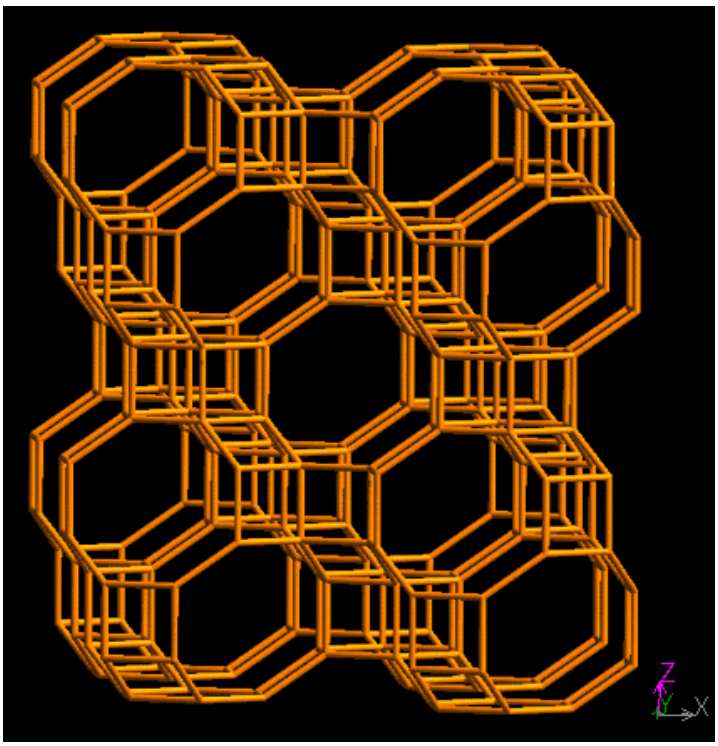

Fig. 2.1.2. 3D framework structure and channel system of SAPO-5 aluminophosphate

2.1.4 VPI-5

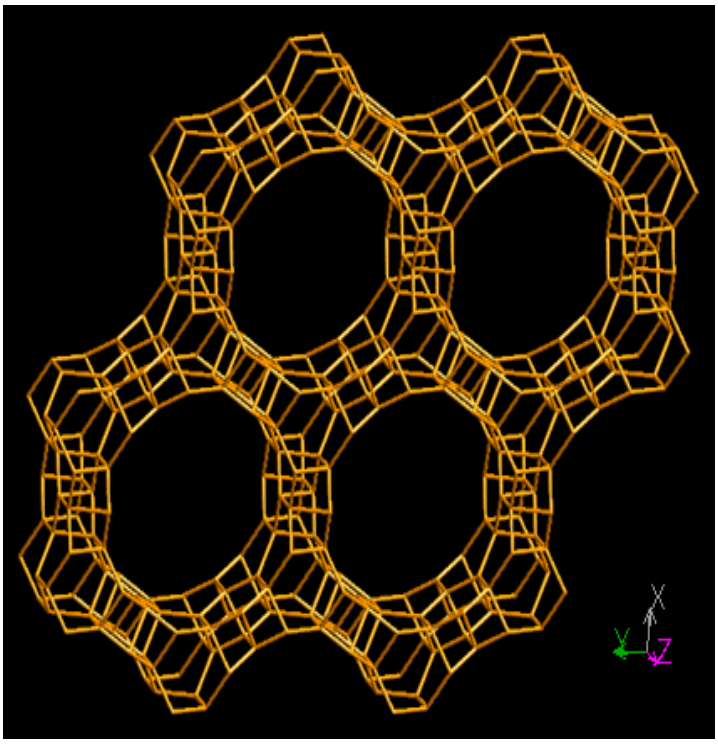

Fig. 2.1.3. 3D framework structure and channel system of VPI-5 aluminophosphate

VPI-5 aluminophosphate has tremendous properties. Its framework structure is VFI type with 18-T ring pore structure and one dimensional channels are present in it (Fig. 2.1.3). Its crystallographic information is as follows:

VPI-5*			
Parameter	**Description**		
Material	VPI-5		
Category	Aluminophosphate		
Molar Composition	$\|(H_2O)_{42}\|$ $[Al_{18}P_{18}O_{72}]$		
Framework Type	VFI		
Crystallography			
Space group	$P6_3/mcm$		
Cell parameters	a = 18.284 Å	b = 18.284 Å	c = 8.589 Å
	α = 90.000°	β = 90.000°	γ=120.000°
Volume	2486.71 $Å^3$		
R_{DLS}	0.0070		
Framework density	14.5 T/1000 $Å^3$		
Channel system	1-dimensional		
Topological density	TD_{10} = 669 TD = 0.562500		
Ring sizes (T atoms)	18 6 4		
Maximum diameter of a sphere			
that can be included	12.03 Å		
that can diffuse along	a: 2.40 Å b: 2.40 Å c: 11.39 Å		

*Framework structure and crystallographic information are obtained from IZA commission.

2.2 Synthesis of aluminophosphate materials

For the present study, hydrothermal synthesis of aluminophosphates was carried out according to the procedures given in the high impact journals however steps for the synthesis and molar composition of the precursor gel was altered in most of the synthesis recipes. The synthesis procedure for different aluminophosphates is described below. Molar composition of all reactants is given in the form of oxide (excepting template) and moles of all the applied reagents for preparation of gel are calculated as per their composition. Inherent amount of water is also considered thus it is needful to subtract this volume of inherent water from the total amount of water in the molar ratio of precursor gel (for all zeotypes). Metal salts used in this study are divalent salts of Co^{2+} and Mn^{2+}.

2.2.1 AlPO-5

This material was synthesised according to the reported procedure [173]. However molar composition of the precursor gel and few of the synthesis steps were altered and are as follows.

Samples of MnAPO-5 and CoAPO-5 were prepared by using triethylamine [132] as the organic structure directing agent or template . On the basis of preliminary experiments, the following gel compositions (Table 2.2.1) were optimized. The metal sources used, were manganese acetate tetrahydrate (Sigma) and cobalt acetate hexahydrate, for MnAPO-5 and CoAPO-5 respectively. In typical synthesis procedure, pseudoboehmite slurry was prepared by mixing pseudoboehmite (75.22% Al_2O_3) with water (1/2 of total water volume) and stirred for two hour. A mixture of phosphoric acid (85% aqueous) in water and mixture of metal acetate (99%) in water were mixed and stirred for homogenization. This mixture of acid-salt and rest of water (1/5), were added drop wise to slurry one after one. Resulting mixture was again stirred for three hour. Then triethylamine (99.8%) was added slowly to mixture and stirred for two hour to get the final gel. AlPO-5 was synthesized without addition of metal salt. In case of CoAPO-5, pseudoboehmite was added directly to mixtures of acid and salt in water. Final gel was transferred to Teflon lined autoclave and heated at 200℃ for 24 h (144 h in case of CoAPO-5). Product was separated from mother liquor, washed, air dried at 80℃ to get as synthesised material and calcinated in air at

500℃ for 10 h. Molar compositions of reaction gel for different catalysts are given in table (2.2.1) below.

Molar compositions of reaction gel

Catalyst	Molar composition	Weight (g)
AlPO-5	$1Al_2O_3/1P_2O_5/2TEA/50H_2O$	9.04/15.36/13.05/50
CoAPO-5	$1Al_2O_3/1P_2O_5/0.01CoO/2TEA/50H_2O$	9.04/15.36/0.73/13.05/50
MnAPO-5	$1Al_2O_3/1P_2O_5/0.01MnO/2TEA/50H_2O$	9.04/15.36/0.163/13.05/50

Table 2.2.1. Molar composition of reaction gel for various catalysts

2.2.2 SAPO-5

Silicoaluminophosphate molecular sieve SAPO-5 and its metal substituted forms (MeSAPO-5) were synthesized hydrothermally using the following gel molar composition (Table 2.2.2.) according to the modified recipe [174]:

Molar compositions of reaction gel

Catalyst	Molar composition	Weight (g)
SAPO-5	$Al_2O_3/P_2O_5/0.3SiO_2/2.0TEA/40H_2O$	9.36/9.43/1.3/14.48/40
CoSAPO-5	$Al_2O_3/P_2O_5/0.3SiO_2/0.1CoO/2.0TEA/40H_2O$	9.36/9.43/1.3/0.18/14.48/40
MnSAPO-5	$Al_2O_3/P_2O_5/0.3SiO_2/0.1MnO/2.0TEA/40H_2O$	9.36/9.43/1.3/0.17/14.48/40

Table 2.2.2. Molar composition of precursor gel for various catalysts

In a typical synthesis, 9.36 g of pseudoboehmite was dispersed into about one half of the total amount of water. The mixture was stirred and another mixture of ortho-phosphoric acid 9.43 ml (85% Aldrich) diluted in water (15 ml) and a mixture of salt in water (5 ml), was added drop by drop to the aluminum slurry under vigorous stirring until a homogeneous mixture was obtained for one hour. 14.48 ml of triethylamine was added and stirring was maintained for 30 min more. After the addition of organic template, the silicon source (fumed silica) was added, keeping the agitation for 30 min more. The pH of gel was maintained at 5 and the resultant

material was transferred into a stainless-steel autoclave, sealed and placed in an oven maintained at 170℃ for 48 h. The obtained solid was filtered, washed with distilled water and dried. Finally, it was calcined at 500℃ in air for 12 h. Following the same recipe as described above, SAPO-5 material (without metal), were prepared without the metal salt.

2.2.3 SAPO-34

Samples of SAPO-34, MnSAPO-34, and CoSAPO-34 were prepared hydrothermally with tetraethyl ammonium hydroxide (TEAOH) as the templating agent. The procedure was adopted from the recipe of Dubois et al. [175]. The following chemicals were used without further purification: ortho-phosphoric acid (85%), aluminum isopropoxide (99.9%), fumed silica (99.9%), tetraethyl ammonium hydroxide (20 wt % aqueous solution), cobalt(II) nitrate (98% hexahydrate), and manganese(II) nitrate (98% hexahydrate).

In typical preparation, aluminum isopropoxide was mixed with tetraethylammonium hydroxide and stirred for about 1.5 hour. Then fumed silica was added to the mixture under vigorous stirring. To this solution, the corresponding metal nitrate, dissolved in 2 ml of water, were added. Finally, phosphoric acid diluted in 4 ml water was added drop wise to this mixture. Stirring continued for another 2 h. The pH of the final gel was 8.0. Molar compositions of final gels were as follow (Table 2.2.3).

Catalyst	Molar composition	Weight (g)
SAPO-34	$Al_2O_3/P_2O_5/0.3SiO_2/TEAOH/40H_2O$	12.17/6.87/0.532/43.89/40
CoSAPO-34	$Al_2O_3/P_2O_5/0.3SiO_2/0.1CoO/TEAOH/40H_2O$	12.1/6.87/0.532/0.08/43.89/40
MnSAPO-34	$Al_2O_3/P_2O_5/0.3SiO_2/0.1MnO/TEAOH/40H_2O$	12.17/6.87/0.53/0.06/43.89/40

Table 2.2.3. Molar composition of precursor gel

To synthesize SAPO-34 material without metal, same recipe was followed without adding the metal salt to the reaction mixture. In all the cases, hydrothermal crystallization was performed at 200℃ for 48 h. After crystallization, the product was

separated from the mother liquor by centrifugation and washed several times with water. The product was then dried at 100℃ overnight. All the as-synthesized samples were slowly heated to 550℃ in flowing air and kept at this temperature overnight in order to remove the organic template. These calcinated samples were then used for catalytic reactions.

2.2.4 VPI-5

This aluminophosphate has pore size more than 12 Å thus attracted most attention during 1990s. However synthesis fact is very different because of its low thermal stability and transformation of this framework to AlPO-8 framework at very low temperature range which makes this zeotype less important in catalytic reactions which are performed at high temperature. Another very important point is that during the synthesis, if temperature sweep of crystallization or increase in temperature rate inside the autoclave (hydrothermal), is not maintained more than 400℃/hour, VPI-5 severely degraded to AlPO-H3 (hydrate-form) which has small pore size and small surface area. In this study, this zeotype was synthesised using the reported recipe by Davis et al. [36] but in the present work hydrated aluminophosphate symmetry (AlPO-H3) was obtained, because maintaining so a high rate of temperature raise for crystallization was not possible. Graphical presentation of synthesis procedure is given in Fig. 2.2.4.

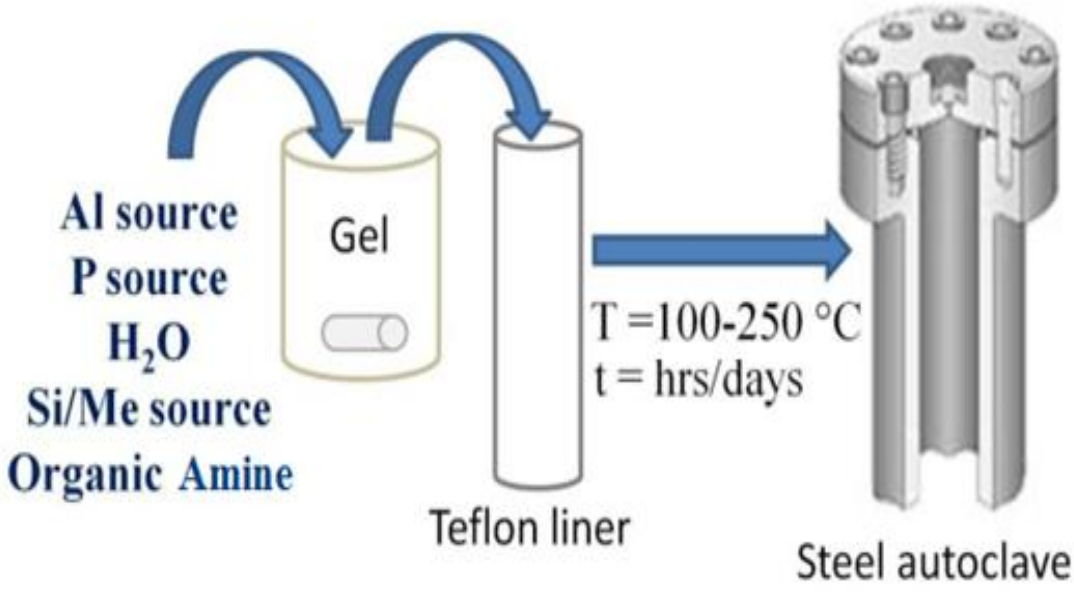

Fig. 2.2.4. Graphical representation of synthesis steps

2.3 Isomorphous substitution

Isomorphous substitution causes acidity in electrically neutral framework of nonsubstituted aluminophosphates. Thus it is needful to insert any divalent transition metal in the framework which will make these materials catalytically more valuable and applicable too. Salts of Cobalt & Manganese were mixed with precursor during synthesis or crystallization of these zeotype materials for isomorphous. Cobalt and manganese were specially selected for the study because their zeotype forms are coloured and substitution can be detected easily by DRS technique. Another most important fact about choosing these atoms was that they have unfilled d-orbitals thus shows different behaviour in catalysis and these orbitals also may cause Lewis acidity in addition to Brønsted acidity. However manganese has poor detection limit as its electronic transition in UV-VIS range are spin forbidden. But diversity in their (metals) coordination may cause redox centres in the framework of zeotypes, which may catalyse redox reactions with its reversible oxidation and reduction properties thus manganese was selected for the study. Mechanism of substitution has been covered in the previous chapter.

2.4 Characterization techniques used in this study

2.4.1 X-Ray Crystallography

Crystallography is the science that examines arrangement of atoms in solids. The word "crystallography" derives from the Greek word crystallon "cold drop, frozen drop", with its meaning extending to all solids with some degree of transparency, and grapho "I write". In July 2012, the United Nations recognised the importance of science of crystallography by proclaiming that 2014 would be the international year of Crystallography. Crystallography is a useful tool for materials scientists. X-ray crystallography is a tool used for identifying the atomic and molecular structure of a crystal, in which the crystalline atoms cause a beam of incident X-rays to diffract into many specific directions. By measuring the angles and intensities of these diffracted beams, a crystallographer can produce a three-dimensional picture of the density of electrons within the crystal. From this electron density, the mean positions of the atoms in the crystal can be determined as well as their chemical bonds, their disorder and various other informations. X-ray

crystallography is still the chief method for characterizing the atomic structure of new materials and in discerning materials that appear similar by other experiments.

Bragg's Equation explains that incoming beam (coming from upper left) causes each scatterer to re-radiate a small portion of its intensity as a spherical wave. If scatterers are arranged symmetrically with a separation d, these spherical waves will be in sync (add constructively) only in directions where their path-length difference 2d sin θ equals an integer multiple of the wavelength λ. In that case, part of the incoming beam is deflected by an angle 2θ, producing a reflection spot in the diffraction pattern. Crystals are regular arrays of atoms, and X-rays can be considered waves of electromagnetic radiation. Atoms scatter X-ray waves, primarily through the atoms' electrons. Just as an ocean wave striking a lighthouse produces secondary circular waves emanating from the lighthouse, so an X-ray striking an electron produces secondary spherical waves emanating from the electron. This phenomenon is known as elastic scattering, and the electron (or lighthouse) is known as the scatterer. A regular array of scatterers produces a regular array of spherical waves. Although these waves cancel one another out in most directions through destructive interference, they add constructively in a few specific directions, determined by Bragg's law:

$$2dsin\theta = n\lambda$$

Here d is the spacing between diffracting planes (Fig 2.4.1), is the incident angle, n is any integer, and λ is the wavelength of the beam. These specific directions appear as spots on the diffraction pattern called reflections. Thus, X-ray diffraction results from an electromagnetic wave (X-ray) impinging on a regular array of scatterers (the repeating arrangement of atoms within the crystal).

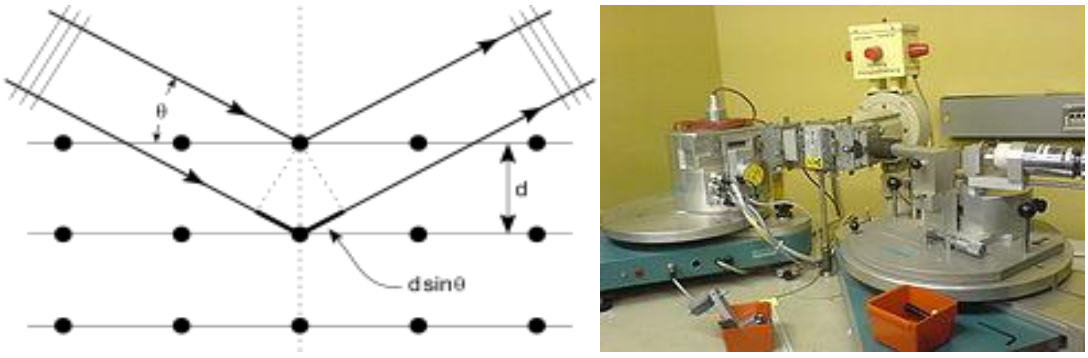

Fig. 2.4.1. Bragg's equation diagram and X-Ray Spectrometer

In general, two methods are applied for crystal structure determination.

(i) Single crystal method

(ii) Powder diffraction method

In a single crystal, the effect of the crystalline arrangement of atoms is often easy to see macroscopically, because the natural shapes of crystals reflect the atomic structure. In addition, physical properties are often controlled by crystalline defects. Mostly, materials do not occur as a single crystal, but in poly-crystalline form (i.e., as an aggregate of small crystals with different orientations). Because of this, the powder diffraction method, which uses diffraction patterns of polycrystalline samples with a large number of crystals (powder), plays an important role in structural determination. In X-ray diffraction measurement, a crystal is mounted on a goniometer and gradually rotated while being bombarded with X-rays, producing a diffraction pattern of regularly spaced spots known as reflections. The two-dimensional images taken at different rotations are converted into a three-dimensional model of the density of electrons within the crystal using the mathematical method of Fourier transforms. In this study samples were scanned using Cu-Kα radiation source and Shimadzu XRD 6000 equipment for X-ray diffraction (XRD).

2.4.2 Fourier transform infrared spectroscopy

Fourier transform infrared spectroscopy (FTIR) is a technique which is used to obtain an infrared spectrum of absorption, emission and photoconductivity of a solid, liquid or gas. An FTIR spectrometer (Fig. 2.4.2) simultaneously collects spectral data in a wide spectral range. This confers a significant advantage over a dispersive spectrometer which measures intensity over a narrow range of wavelengths at a time. The term ‘Fourier transform infrared spectroscopy’ originates from the fact that a Fourier transform (a mathematical process) is required to convert the raw data into the actual spectrum. Infrared light is guided through an interferometer and then through the sample (or vice versa). A moving mirror inside the apparatus alters the distribution of infrared light that passes through the interferometer. The signal directly recorded, called an "interferogram", represents light output as a function of mirror position. A data-processing technique called Fourier transform turns this raw data into the desired result (the sample's spectrum) which is a light output as a function of infrared wavelength (or equivalently, wave number). The infrared spectrum of a sample is

recorded by passing a beam of infrared light through the sample. When the frequency of the IR is the same as the vibrational frequency of a bond, absorption occurs. Examination of the transmitted light reveals how much energy was absorbed at each frequency (or wavelength). This can be achieved by scanning the particular wavelength range. Alternatively, the whole wavelength range is measured at once using a Fourier transform instrument and then a transmittance or absorbance spectrum is generated using a dedicated procedure. Analysis of the position, shape and intensity of peaks in this spectrum reveals details about the molecular structure of the sample.

Fig. 2.4.2. FTIR spectrometer

A molecule can vibrate in many ways, and each way is called a vibrational mode. For molecules with N number of atoms in them, linear molecules have 3N-5 degrees of vibrational modes, whereas nonlinear molecules have 3N-6 degrees of vibrational modes (also called vibrational degrees of freedom). As an example H_2O, a non-linear molecule, will have 3×3-6=3 degrees of vibrational freedom or modes. Simple diatomic molecules have only one bond and only one vibrational band. If the molecule is symmetrical, e.g. N_2, the band is not observed in the IR spectrum, but only in the Raman spectrum. Asymmetrical diatomic molecules, e.g. CO, absorb in

the IR spectrum. More complex molecules have many bonds and their vibrational spectra are correspondingly more complex, i.e. big molecules have many peaks in their IR spectra. Solid samples can be prepared in a variety of ways. One common method is to crush the sample with an oily mulling agent (usually Nujol) in a marble or agate mortar, with a pestle. A thin film of the mull is smeared onto salt plates and measured. The second method is to grind a quantity of the sample with a specially purified salt (usually potassium bromide) finely (to remove scattering effects from large crystals). This powder mixture is then pressed in a mechanical press to form a translucent pellet through which the beam of the spectrometer can pass.

In present study Shimadzu FT-IR spectrophotometer (Perkin-Elmer spectrumRX-IFTIR) equipped with a narrowband MCT detector was used for FTIR analysis of zeotype materials and reactions product of catalysis.

2.4.3 Nuclear Magnetic Resonance Spectroscopy

It is one of the principal techniques used to obtain physical, chemical, electronic and structural information about molecules. It is a powerful technique that can provide detailed information on the topology, dynamics and three-dimensional structure of molecules in solution and the solid state. Many scientific techniques exploit NMR phenomena to study molecular physics, crystals and non-crystalline materials through NMR spectroscopy. NMR is also routinely used in advanced medical imaging techniques, such as in magnetic resonance imaging (MRI).

Nuclear magnetic resonance (NMR) is a physical phenomenon in which nuclei in a magnetic field absorb and re-emit electromagnetic radiation. This energy is at a specific resonance frequency which depends on the strength of the magnetic field and the magnetic properties of the isotope of the atoms. In practical applications, the frequency is similar to VHF and UHF television broadcasts (60–1000 MHz). All isotopes that contain an odd number of protons and/or of neutrons have an intrinsic magnetic moment and angular momentum. In other words, a nonzero spin, while all nuclides with even numbers of both have a total spin of zero. A non-zero spin is thus always associated with a non-zero magnetic moment (μ). It is this magnetic moment that allows the observation of NMR absorption spectra caused by transitions between nuclear spin levels in a applied magnetic field. When spin state of a proton go down

to the ground state called relaxation, emits radiations which can be plotted to produce NMR spectra. The most commonly studied nuclei are ^{1}H and ^{13}C.

Fig. 2.4.3. NMR spectrometer

A key feature of NMR is that the resonance frequency of a particular substance is directly proportional to the strength of the applied magnetic field. It is this feature that is exploited in imaging techniques; if a sample is placed in a non-uniform magnetic field then the resonance frequencies of the sample's nuclei depend on where in the field they are located. The principle of NMR usually involves two sequential steps:

- The alignment (polarization) of the magnetic nuclear spins in an applied, constant magnetic field H_0.
- The perturbation of this alignment of the nuclear spins by employing an electro-magnetic, usually radio frequency (RF) pulse. The required perturbing frequency is dependent upon the static magnetic field (H_0) and the nuclei of observation.

In present study Avance-II (Bruker) 400 MHz (Fig. 2.4.3) was used for analysis of reaction product of catalysis. Chemical shifts (δ) are reported in ppm relative to internal TMS. Multiplicities such as singlet, doublet, and triplet if present are reported in their spectra.

2.4.4 Diffuse Reflectance Spectroscopy (DRS)

Diffuse reflectance is an excellent sampling tool for powdered or crystalline materials. Diffuse reflection is the reflection of light from a surface such that an incident ray is reflected at many angles rather than at just one angle as in the case of specular reflection. An illuminated ideal diffuse reflecting surface will have equal luminance from all directions which lie in the half-space adjacent to the surface (Lambertian reflectance). A surface built from a non-absorbing powder such as plaster, or from fibers such as paper, or from a polycrystalline material such as white marble, reflects light diffusely with great efficiency. If the diffuse surface is coloured, the reflected light is also colored, resulting in similar coloration of surrounding objects.

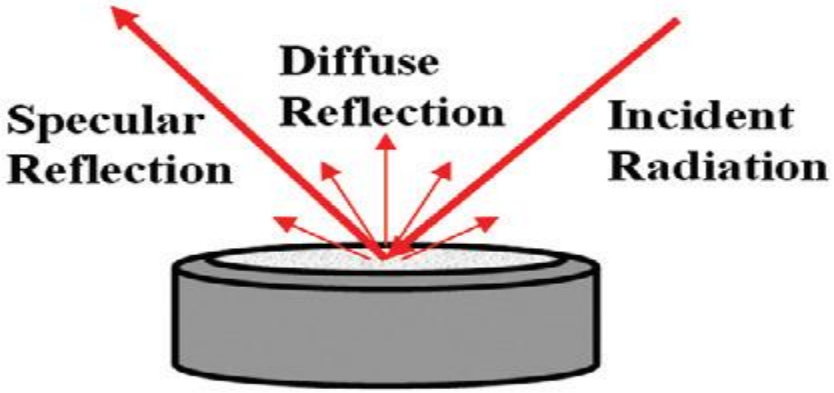

Fig. 2.4.4. Principle of diffuse reflectance

Diffuse reflectance relies upon the focused projection of the spectrometer beam into the sample where it is reflected, scattered and transmitted through the sample material. The back reflected, diffusely scattered light (some of which is absorbed by the sample) is then collected by the accessory and directed to the detector optics. Only the part of the beam that is scattered within a sample and returned to the surface is considered to be diffuse reflection (Fig. 2.4.4).

Usually, the sample must be ground and mixed with a non-absorbing matrix such as KBr. The sample to matrix ratio should be between 1 to 5% (by weight). Diluting ensures a deeper penetration of the incident beam into the sample which increases the contribution of the scattered component in the spectrum and minimizes the specular reflection component. A Kubelka-Munk conversion can be applied to a diffuse reflectance spectrum expressed as follows:

$$f(R) = \frac{(1-R)^2}{2R} = \frac{k}{s}$$

Where: R is the absolute reflectance of the sampled layer, k is the molar absorption coefficient and s is the scattering coefficient. The Kubelka-Munk equation creates a linear relationship for spectral intensity relative to sample concentration.

For the analysis of powder, the following procedure is recommended; Powder sample (5 mg) is placed (200-400 mg of KBr) in a vial and shake for 30 seconds. Slide the sample holder (vial) into the accessory and collect spectrum using KBr as blank. Convert the raw diffuse reflectance spectrum to Kubelka-Munk and plot the obtained intensity with wavelength to produce DRS spectra.

2.4.5 BET-Surface area analysis

Brunauer–Emmett–Teller (BET) theory aims to explain the physical adsorption of gas molecules on a solid surface and serves as the basis for an important analysis technique for the measurement of the specific surface area of a material. In 1938, Stephen Brunauer, Paul Hugh Emmett, and Edward Teller published the first article about the BET theory in the Journal of the American Chemical Society. The concept of the theory is an extension of the Langmuir theory, which is a theory for monolayer molecular adsorption to multilayer adsorption with the following hypotheses: (a) gas molecules physically adsorb on a solid in layers infinitely; (b) there is no interaction between each adsorption layer; and (c) the Langmuir theory can be applied to each layer. The resulting BET equation is:

$$\frac{1}{v\left[(p_0/p)-1\right]} = \frac{c-1}{v_{\mathrm{m}}c}\left(\frac{p}{p_0}\right) + \frac{1}{v_m c}, \qquad (1)$$

Where $\boldsymbol{p_0}$ and p are the equilibrium and the saturation pressure of adsorbates at the temperature of adsorption, υ is the adsorbed gas quantity (for example, in volume units), and υ_m is the monolayer adsorbed gas quantity. C is the BET constant,

$$c = \exp\left(\frac{E_1 - E_L}{RT}\right), \qquad (2)$$

Where E_1 is the heat of adsorption for the first layer, and E_L is that for the second and higher layers and is equal to the heat of liquefaction.

Equation (1) is an adsorption isotherm and can be plotted as a straight line with $1/\upsilon[(p_0/p)-1]$ on the y-axis and $Ø = p_\circ / p$ on the x-axis according to experimental results. This plot is called a BET plot (Fig 2.4.5).

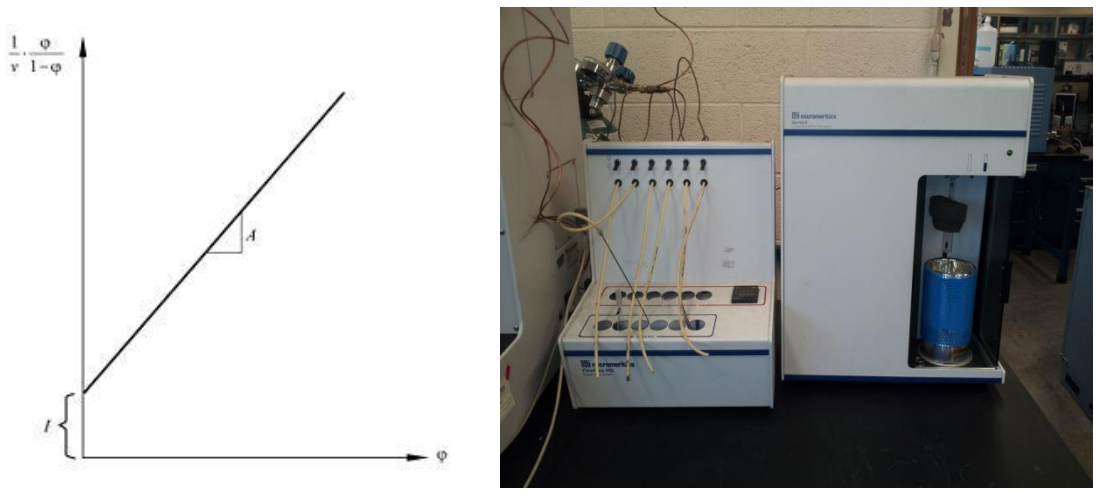

Fig. 2.4.5. Adsorption isotherm plot(left) and instrument (right)

The linear relationship of this equation is maintained only in the range of $0.05 < p_0/p < 0.35$. The value of the slope A and the y-intercept I of the line are used to calculate the monolayer adsorbed gas quantity υ_m and the BET constant C. The following equations can be used:

$$v_m = \frac{1}{A + I} \qquad (3)$$

$$c = 1 + \frac{A}{I}. \qquad (4)$$

The BET method is widely used in surface science for the calculation of surface areas of solids by physical adsorption of gas molecules. Currently, there are

two basic principles for testing BET surface area. The first one called flowing gas principle (like F-Sorb 2400CE principle) and the second is static volumetric principle (like V-Sorb 2800TP principle). The first one use helium and nitrogen mixed gas as adsorbate, and the helium works as dosing gas, the nitrogen as adsorption gas. The static volumetric principle must have two gas cylinders, one is helium and another is nitrogen, must be upper than 99.99% purity. Prior to any measurement the sample must be degassed to remove water and other contaminants before the surface area can be accurately measured. Samples are degassed in a vacuum at high temperatures. The highest temperature possible that will not damage the sample's structure is usually chosen in order to shorten the degassing time. IUPAC recommends that samples be degassed for at least 16 hours to ensure that unwanted vapors and gases are removed from the surface of the sample. Generally, samples that can withstand higher temperatures without structural changes have smaller degassing times. A minimum of 0.5 g of sample is required for the BET to successfully determine the surface area. In present study Autosorb 2120 BET analyzer (Fig. 2.4.5) was used for surface area analysis.

2.4.6 Scanning Electron Microscope

A scanning electron microscope is a type of electron microscope that produces images of a sample by scanning it with a focused beam of electrons. The electrons interact with atoms in the sample, producing various signals that can be detected and that contain information about the sample's surface topography and composition. The electron beam is generally scanned in a raster scan pattern, and the beam's position is combined with the detected signal to produce an image. SEM can achieve resolution better than 1 nanometre. Specimens can be observed in high vacuum, in low vacuum, in wet conditions (in environmental SEM), and at a wide range of cryogenic or elevated temperatures. The most common mode of detection is by secondary electrons emitted by atoms excited by the electron beam. On a flat surface, the plume of secondary electrons is mostly contained by the sample, but on a tilted surface, the plume is partially exposed and more electrons are emitted. By scanning the sample and detecting the secondary electrons, an image displaying the topography of the surface is created.

For conventional imaging in the SEM, specimens must be electrically conductive, at least at the surface, and electrically grounded to prevent the accumulation of electrostatic charge at the surface. Metal objects require little special preparation for SEM except for cleaning and mounting on a specimen stub.

Fig. 2.4.6. Scanning Electron Microscope

Nonconductive specimens tend to charge when scanned by the electron beam, and especially in secondary electron imaging mode, this causes scanning faults and other image artefacts. They are therefore usually coated with an ultra-thin coating of electrically conducting material, deposited on the sample either by low-vacuum sputter coating or by high-vacuum evaporation. Conductive materials currently used for specimen coating include gold, gold/palladium alloy, platinum, osmium, iridium, tungsten, chromium, and graphite. In the present study, the samples were analyzed using JEOL JSM-6390LV microscope (Fig. 2.4.6).

In a typical SEM, an electron beam is thermionically emitted from an electron gun fitted with a tungsten filament cathode. The electron beam, which typically has an energy ranging from 0.2 keV to 40 keV, is focused by one or two condenser lenses to a spot about 0.4 nm to 5 nm in diameter. The beam passes through pairs of scanning coils or pairs of deflector plates in the electron column, typically in the final lens, which deflect the beam in the x and y axes so that it scans in a raster fashion over a rectangular area of the sample surface. When the primary electron beam interacts with the sample, the electrons lose energy by repeated random scattering and absorption within a teardrop-shaped volume of the specimen known as the interaction volume, which extends from less than 100 nm to approximately 5 μm into the surface. The size of the interaction volume depends on the electron's landing energy, the atomic number of the specimen and the specimen's density. The energy exchange between the electron beam and the sample results in the reflection of high-energy electrons by elastic scattering, emission of secondary electrons by inelastic scattering and the emission of electromagnetic radiation, each of which can be detected by specialized detectors. The beam current absorbed by the specimen can also be detected and used to create images of the distribution of specimen current.

2.4.7 Energy dispersive spectroscopy (EDS)

Energy dispersive spectroscopy is an analytical technique used for the elemental analysis or chemical characterization of a sample. EDS accessory is equipped within the SEM instrument which produces images for elemental composition of material under SEM analysis simultaneously. It relies on the investigation of an interaction of some source of X-ray excitation and sample. Its characterization capabilities are due to the fundamental principle that each element has a unique atomic structure allowing unique set of peaks on its X-ray spectrum. To stimulate the emission of characteristic X-rays from a specimen, a high-energy beam of charged particles such as electrons or protons, or a beam of X-rays, is focused into the sample being studied. At rest, an atom within the sample contains ground state (or unexcited) electrons in discrete energy levels or electron shells bound to the nucleus. The incident beam may excite an electron in an inner shell, ejecting it from the shell while creating an electron hole where the electron was. An electron from an outer higher-energy shell then fills the hole, and the difference in energy between the

higher-energy shell and the lower energy shell may be released in the form of an X-ray. The number and energy of the X-rays emitted from a specimen can be measured by an energy-dispersive spectrometer. As the energy of the X-rays is characteristic of the difference in energy between the two shells, and of the atomic structure of the element from which they were emitted, this allows the elemental composition of the specimen to be measured.

The determination of bulk element composition of mica minerals is of importance in many aspects of synthesized materials, their characterization and applications. This information is used to verify the synthesis formulation, the bulk silica/ alumina ratio, the cation concentration, degree of ion exchange and detection of contaminant element. EDS spectra were measured on JEOL-JED-2300 system.

2.5 Catalytic Study

All the zeotype forms were used as catalyst in various reactions to test their catalytic efficiency. Zeotypes are referred as catalyst hereinafter. All the catalyst materials were calcinated in air prior to their use as catalyst.

2.5.1 Synthesis procedure of 2,4,5-triphenyl-1H-imidazole

For typical reaction (Scheme 2.5.1.), 1 mmol of benzil, 1mmol of p-hydroxybenzaldehyde, 5 mmol of ammonium acetate and 100 mg of catalyst was taken in round bottom flask fitted with a condenser and magnetic stirrer device. Flask was heated to 110℃ with stirring. Completion of reaction was observed by TLC, however after some time reaction mixture gets solidified and no further reaction proceeds. Reaction mixture was cooled down and 50 ml ice water was mixed. Solid imidazole precipitates out, filtered, washed with distilled water and after drying this crude product, dissolved in warm ethanol to recover catalyst by filtration and finally crude product was recrystallized by aqueous ethanol to afford pure product. Product was analysed by ^{1}HNMR (400 MHz, DMSO-d_6) and FTIR. Isolated (recrystallized) product was taken as the weight of product and thus on this basis product yield (wt %) was measured with respect to the total weight of reactants which is as follows:

$$\textbf{Product yield}\ (\%) = \frac{\textbf{Actual yield}(\textbf{g})}{\textbf{Theoretical yield}\ (\textbf{g})} \times \mathbf{100}\%$$

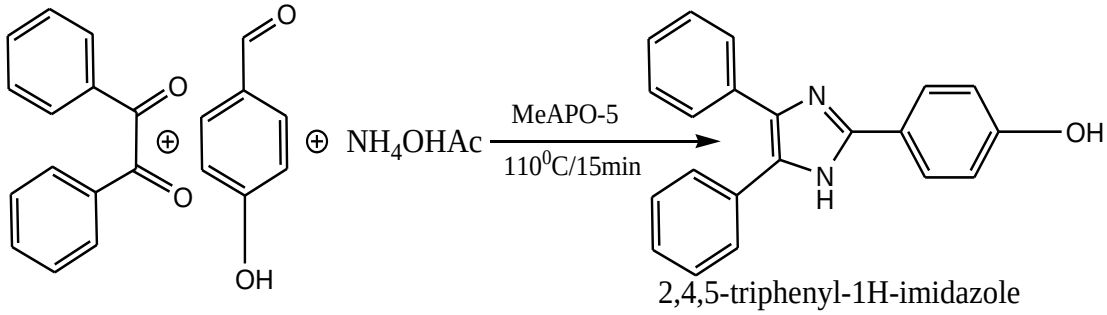

2,4,5-triphenyl-1H-imidazole

(Scheme 2.5.1)

2.5.2 Synthesis procedure of 6-nitro-2,3-diphenylquinoxaline

Benzil (1 mmol), 4-nitrobenzene-1,2-diamine (1mmol) and 120 mg of catalyst were taken in a round bottom flask fitted with a condenser. 5 ml of ethanol was taken as solvent. Reaction mixture was stirred with heating at 323K (Scheme 2.5.2). After completion of reaction (by TLC), reaction mixture was cooled down and solvent was evaporated by vacuum filtration. Then 20 ml of dichloromethane is added to the obtained solid to separate catalyst. Dichloromethane was evaporated and crude product was recrystallized using ethanol. Reaction product was characterised by NMR and FTIR techniques.

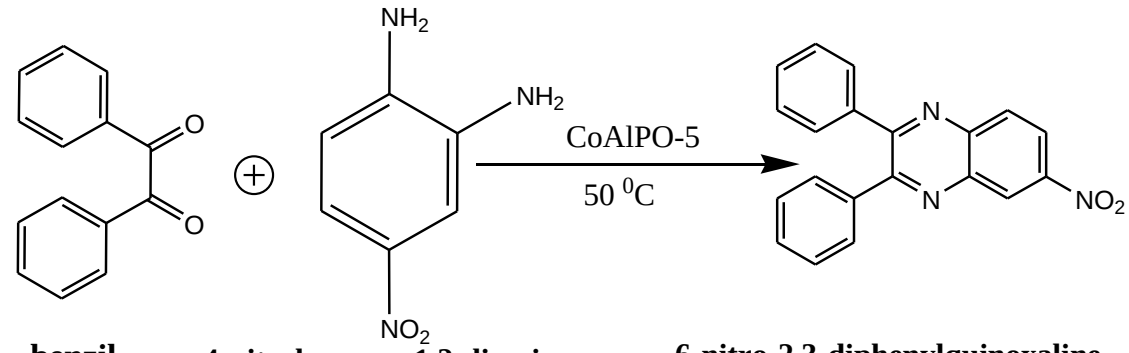

benzil **4-nitrobenzene-1,2-diamine** **6-nitro-2,3-diphenylquinoxaline**

(**Scheme 2.5.2)**

2.5.3 Esterification reaction

Esterification of acetic acid with sec-butanol was studied over zeotypes. Freshly activated catalyst (100 mg dried at 120 ℃ for 2 h in an oven), 0.15 mol of acetic acid (Merck, 99.8%), 0.05 mol of sec-butanol (Merck, 98%) were taken in a round bottom flask. Temperature was then slowly raised to 100-170℃ and maintained at the desired temperature during the specified reaction periods (1-8 h).

The reaction products were collected from the round bottom flask and analyzed by NMR and FTIR. The catalyst was then washed with water and activated for the next experiments. Reaction scheme is presented in scheme 2.5.3.

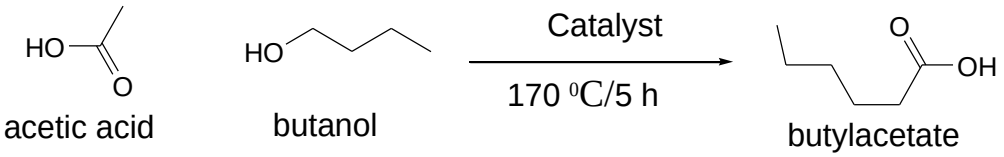

(Scheme 2.5.3)